Bull. Min. Res. Exp. (2018) 157: 39-57

Bulletin of the Mineral Research and Exploration

http://bulletin.mta.gov.tr

Post-Glacial Terraces of The Marmara Sea and Water Exchange Periods

Vedat EDİGER[a*], Emin DEMİRBAĞ[b], Semih ERGİNTAV[c], Sedat İNAN[d] and Ruhi SAATÇILAR[e]

[a]*The Scientific and Technological Research Council of Turkey, Marmara Research Center, Earth and Marine Sciences Institute, Gebze-Kocaeli, Turkey. orcid.org/0000-0003-4388-7951*

[b]*Istanbul Technical University, Department of Geophysics, Maslak-Istanbul, Turkey. orcid.org/0000-0001-8448-8741*

[c]*Boğazici University Kandilli Observatory Earthquake Research Institute Department of Geodesy Çengelköy-Istanbul/Turkey. orcid.org/0000-0001-5094-6599*

[d]*Saudi Aramco, EXPEC Advanced Research Center, Dhahran 31311, Saudi Arabia. orcid.org/0000-0001-5639-6831*

[e]*Department of Geophysical Engineering, Faculty of Engineering, Sakarya University, Sakarya 54187, Turkey. orcid.org/0000-0001-6739-1702*

Research Article

Keywords:
Marmara Sea, morphology, marine terraces, sea-level changes, paleo-lagoon.

ABSTRACT

Semi enclosed Marmara Sea is a passage between the Aegean Sea (Northeastern Mediterranean Sea) and the Black Sea. The Marmara Sea is connected to the Black Sea and Aegean Sea through the İstanbul Strait (Bosphorus) and Çanakkale Strait (Dardanelles), respectively. Despite the fact that the late Pleistocene-Holocene connections between the seas have been explored by many scientists, there are still uncertainties about the nature and timing of the connections. Within the scope of this study, a new approach has been displayed for post-glacial connections between the Black Sea, Marmara Sea and Aegean Sea. This study is based on 80 shallow seismic reflection lines, multibeam bathymetric data and 15 short gravity cores collected from the northeastern shelf of the Marmara Sea (between Silivri and Golden Horn). The sea bottom and sub-bottom morphology have a highly chaotic structure at the exit of the Büyükçekmece/Küçükçekmece lagoons and further east near the Marmara- İstanbul Strait junction. This chaotic bottom and sub-bottom surface morphologies are mainly controlled by the structure of the basin, current regime of the shelf, coastal drainage systems and by the sea/lake water level changes controlled by climate and the sill depths of the two straits, which in turn determined the water exchange between the seas. The sedimentological interpretation of the seismic reflection profiles and core sediments have allowed us to distinguish five stratigraphic units (S1-S5) and four sedimentary layers (A-D) over the acoustic basement. The lower stratigraphic unit and sedimentary layer are separated from the overlying acoustic basement by a chaotic to parallel and by a high amplitude seismic reflector. Seaward dipping units of the acoustic basement are inferred to be the seaward continuation of the Oligocene–Upper Miocene units widely exposed on land. The presence of three different marine terraces distinguished (T1-T3) along the northeastern shelf of the Marmara Sea have been associated with the six different curves of the post-glacial sea-level changes. From statistical point of view, the most significant terraces occur from -78 m to -80 m (T1), -58 m to -62 m (T2) and -28 m to -32 m at (T3). Considering the global sea level curves, these terraces can be dated 9.25, 12.25 and 13.75 Cal kyr BP, respectively.

Received Date: 09.10.2017
Accepted Date: 27.02.2018

1. Introduction

The Marmara Sea is an inland sea with a surface area of approximately 11,350 km^2 which is connected to the Black Sea and the Mediterranean Sea through the İstanbul Strait and Çanakkale Strait respectively (Figure 1). The Istanbul Strait is about 30 km long and its width varies between 0.7 and 3.7 km with water depth varies from 36 to 124 m. Çanakkale Strait is about 61 km long and 1-6 km wide with mean water depth of 55 m (Beşiktepe et al., 1994; Polat and Tuğrul, 1996).

* *Corresponding author: Vedat EDİGER, vedat.ediger@tubitak.gov.tr*
http://dx.doi.org/ 10.19111/bulletinofmre.401208

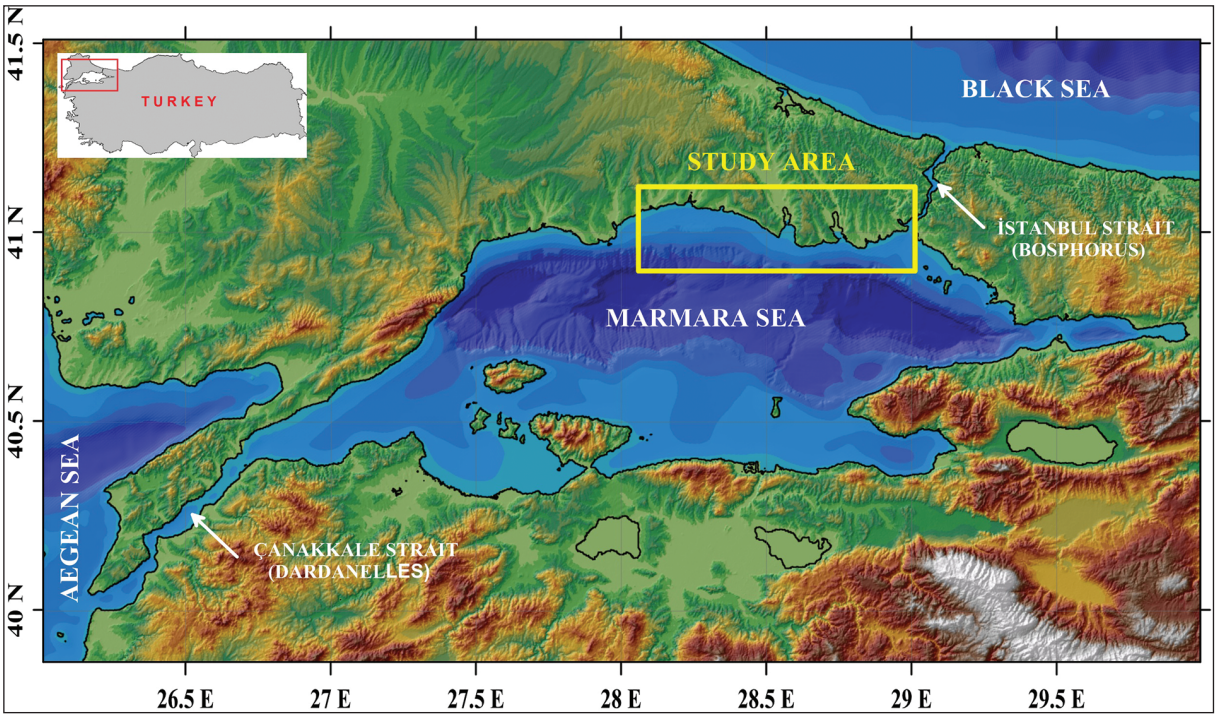

Figure 1- Sea bottom morphology (General Bathymetric Chart of the Oceans; GEBCO), topography of landmass (Shuttle Radar Topography Mission; SRTM) and location of the study area. Coastline data are taken from the Istanbul Metropolitan Municipality.

The Marmara Sea and the strait system regulate the oceanographic conditions and sea-level differences between the Black Sea and the Mediterranean Sea. At present, the Black Sea level is high (~30 cm above the Marmara Sea) due to high discharge of major European and Asian rivers, resulting in outflow through the Istanbul Strait (net outflow is ~300 km^3/yr) (Ünlüata et al., 1990; Oğuz et al., 1990; Beşiktepe et al., 1994). The present water exchange across the Çanakkale and İstanbul Straits occurs as a two-layer flow. A cooler and lower salinity (‰ 17-20) Black Sea water exits southward at the surface while warmer and higher salinity (‰ 38-39) Mediterranean Sea water flows northward at depth through the straits (Polat and Tuğrul, 1996; Özsoy et al., 2001). The water column of the Marmara Sea is characterized by two distinct layers with different temperature and salinity levels: the upper layer (salinity <25psu) and the deeper layer (salinity=38.7psu), separated by a steep halocline located between 20 – 25 m (Beşiktepe et al., 1994). Major rivers flow into the Marmara Sea only from the south and discharge ~$2.2x10^6$ tons/yr of suspended sediment (EIE, 1993). The Marmara Sea has strong surface and relatively strong bottom currents (Beşiktepe et al., 1994) and a small tidal range (8-10 cm, DAMOC, 1971; Alpar and Yüce, 1998).

The reconnections among the Black, Marmara and Mediterranean Seas after the Last Glaciation have been discussed in recent literature. Various scenarios have been proposed for the modes and periods of the connections e.g., Ryan et al. (1997); Gökaşan et al. (1997); Görür et al. (2001); Aksu et al. (2002*a, b* and *c*); Kaminski et al. (2002); Myers et al. (2003); Polonia et al. (2004); Major et al. (2006); Hiscott et al. (2002, 2007 and 2008); Meriç and Algan (2007); Eriş et al. (2007 and 2008); Martin et al. (2007); McHugh et al. (2007); Çağatay et al. (2000, 2003,2009, 2015). Myers et al. (2003) examined the catastrophic flood hypothesis through the İstanbul Strait proposed by Ryan et al. (2003) by means of a series of simple hydraulic calculations to investigate some of the questions associated with the Holocene reconnection of the Black Sea with the Mediterranean Sea through the Turkish Straits System. The same hydraulic model was also used to elucidate the more traditional connection hypothesis of continuous freshwater outflow from the Black Sea, and slowly increasing saline water inflow from the Mediterranean Sea beginning around 8-9 Cal kyr BP (Myers et al., 2003). According to an alternative outflow hypothesis, the Black Sea level was at -40 m (i.e., the bedrock sill depth in the Istanbul Strait), Black Sea waters were cascading down slope into the rising Marmara Sea from 10 to 9 Cal kyr BP and finally constructing the

outflow delta at the southern exit of the strait (Hiscott et al., 2002; Aksu et al., 2002*b*). However, the same delta was claimed to have been formed by sediments transported by the Kurbağalıdere River during the middle Holocene (Eriş et al., 2007).

The main objective of this study is to investigate the Late Quaternary sub-marine terraces on the northern shelf of the Marmara Sea between Silivri and Golden Horn and its implications for sea-level change (Figure 1). We also would like to identify the effects of the sea-level rise on the sediment supply and paleo-oceanographic conditions of the region using sedimentological, geochemical, seismic reflection and bathymetric data.

Four different chronostratigraphic sedimentary layers and five different seismic units have been distinguished over the acoustic basement in the Northern Shelf of the Marmara Sea. Three distinct terraces are clearly identified in the interpreted seismic reflection profiles. The latest connection between the Mediterranean and Marmara Seas was established as the sea-level reached the sill depth of the Çanakkale Strait. At the end of this wet period, Mediterranean saline water invaded the Marmara Sea bottom and gradually established anoxic conditions (Çağatay et al., 1999 and 2000). Further rise of the sea-level during the next warm period reached the depth of the Istanbul Strait and the latest connection between the Marmara, Black and Aegean Seas was established.

2. Materials and Methods

In this study, geophysical (shallow seismic and bathymetric) and sedimentological (gravity cores) data collected from the northeastern shelf of the Marmara Sea were used. Total of 94 seismic reflection profiles with 1100 km length were acquired during the cruise of the R/V Koca Piri Reis in October 2007 and fifteen gravity cores were collected during the cruise of the R/V Arar in March 2008 (Figure 2).

Continuous seismic reflection surveying was carried out by using a standard side mounted (SeaBed 3010 Mp; frequency: 3-7 kHz) and a deep-towed chirp (GeoChirp II Sub-bottom Profiler; frequency: 1 kHz-12 kHz) sub-bottom profilers. The seismic reflection data along 80 lines (Figure 2) are used to map the sub-bottom features such as total sediment thickness and paleo-topography of the acoustic basement. In interpretation of the reflection patterns in the seismic reflection data, methods defined by Mitchum et al. (1977); Vail et al. (1977); Brown and Fisher (1980); Sangree and Widmier (1977); Badley (1985) and Boggs (1987) were followed. Depth conversions were made using a sound velocity of 1500 m/s for the sea water depth and 1600 m/s for the Late Quaternary sediment thickness (Ediger et al., 1993; Okyar et al., 1994). A Differential Global Positioning System (DGPS) was used for navigation during the cruises.

Total of 12.579 surface depth values (in meter) of the acoustic basement with 5 m interval from a total of

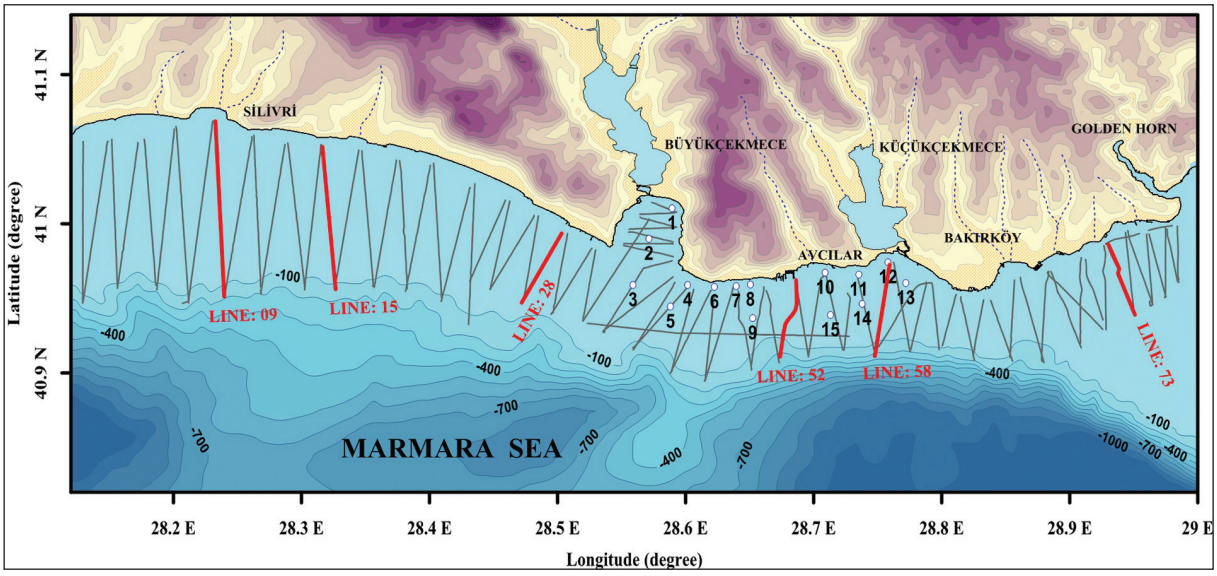

Figure 2- General bathymetry (100 m intervals) (General Bathymetric Chart of the Oceans; GEBCO), coastal topography (20 m intervals) (Shuttle Radar Topography Mission; SRTM), coastal drainage system, shallow seismic lines and sediment core locations are shown along the northeastern Marmara shelf. Bold red lines indicate seismic sections and bold white dots indicates sediment core locations.

40 interpreted shallow seismic reflection profiles are sampled to find the prominent topographic features and determine the most significant terraces in the northeastern shelf of the Marmara Sea. The clarity and the coverage area (depth intervals) of the terraces along the seismic reflection profiles have been considered in determining the number of depth measurements on each of the terraces.

A total of 15 sediment cores were obtained using a standard gravity corer along the inner Marmara shelf area between the Büyükçekmece and Küçükçekmece bays where the maximum water depth is 76 m (Figure 2). The cores were opened in the laboratory for visual observation of lithology and sedimentary structure. For this study, 12 sub-samples were selected based on colour, grain size, shell contents and layers (A1, A2 and A3) within the top layers of the cores (Figure 3). Each sample was dried and powdered for geochemical analysis. Approximately 80 mg of the samples were weighed for TOC analysis using a Rock-Eval 6 Pyrolysis device at the TÜBİTAK Marmara Research Center, Environmental and Petroleum Geochemistry Lab (Figure 3).

A chronology was established based on ^{14}C analysis from five molluscs and one *Lithothamnium* samples (Figure 3; Unit B). Radiocarbon analysis was carried

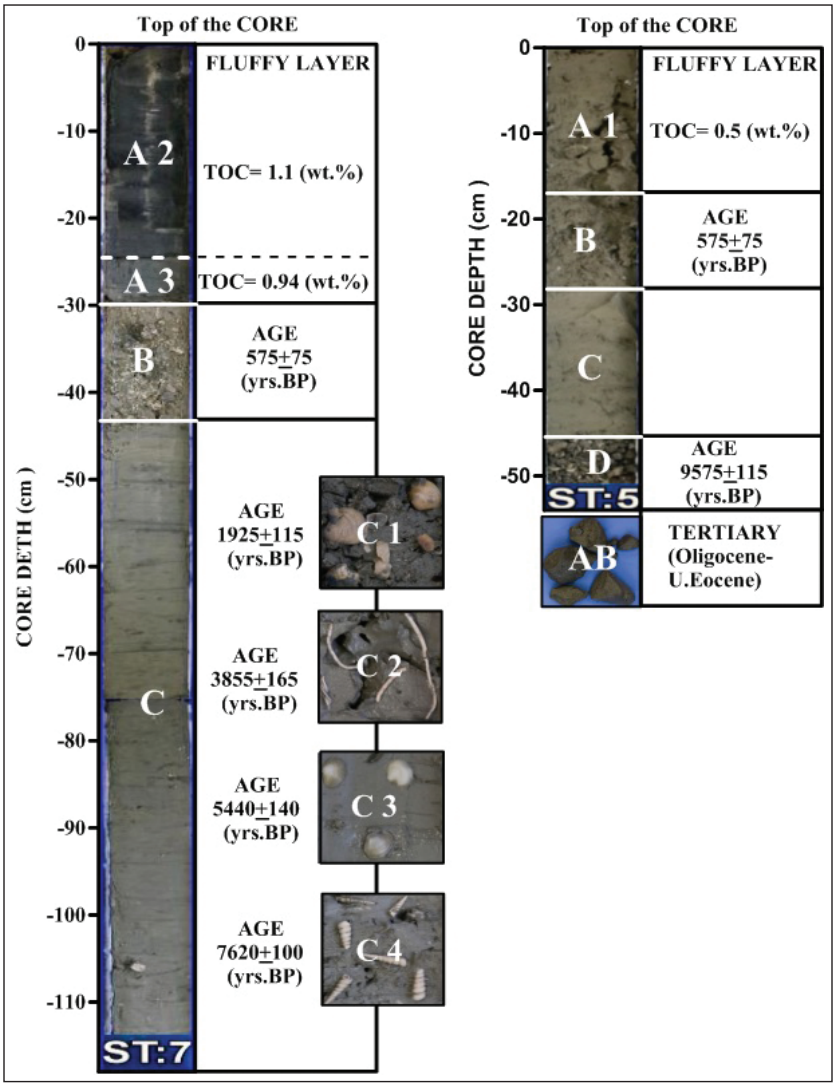

Figure 3- The generalized columnar section showing the units and subunits distinguished by the examination of 15 gravity cores (St. 1-15). A (subunits: A1-A3), B, C (subunits: C1-C4) and D are the main Late Quaternary sediment units and AB is the rocky acoustic basement. TOC values of the A1-A3 and age of the B, C (subunits: C1-C4) and D units are given at figure.

out at the NOSAMS Facility at Woods Hole, MA. The age variability of the sediments is reported as both calibrated (Keven, 2002) years BP and radiocarbon years BP (Figure 3). Finally, the ages were converted to calendar years. CALIB makes the conversion from radiocarbon age to calibrated calendar years by calculating the probability distribution of the sample's true age. (Stuiver and Reimer, 1993).

Four (bivalve, gastropod and *Lithothamnium*) samples were cleaned powdered and analysed for oxygen isotope values ($\delta^{18}O$). Oxygen isotope analysis was conducted using EA-GC/IRMS (Micromass UK) at the TÜBİTAK Marmara Research Center, Environmental and Petroleum Geochemistry Lab. IAEA standards were used to calibrate the instrument. Pore waters were extracted from the same depths as the samples (bivalve, gastropod and *Lithothamnium*) collected for the radiocarbon dating analyses. Pore-water salinity measured by salinometer (WTW, ph/Cond 340i).

3. Results and Interpretations

3.1. Sea Bottom Topography and Depth Analysis

The studied shelf area becomes narrower and deeper from west to east direction (Figure 4). Most significant four depth intervals of the sea bottom topography (between -10m and -12m, -24 m and -26m, -54 and -58m and -76 and -80 m) along the shelf were distinguished as a result of data interpretation by using the depth distribution bar-graphs shown in figure (4). It can be clearly seen that the most predominant depth range along the shelf is between -54m and -58m. Morphological characteristics varies considerably from west to east, which are likely to be due to the structural characteristics, distance to the NAF, coastal morphology, bottom current system and coastal sedimentary processes.

3.2. Seismic Stratigraphy and Sediment Thickness

According to the basic seismic stratigraphic principles, three distinct main boundary reflector surfaces (R1-R3) and two unconformity surfaces (U1

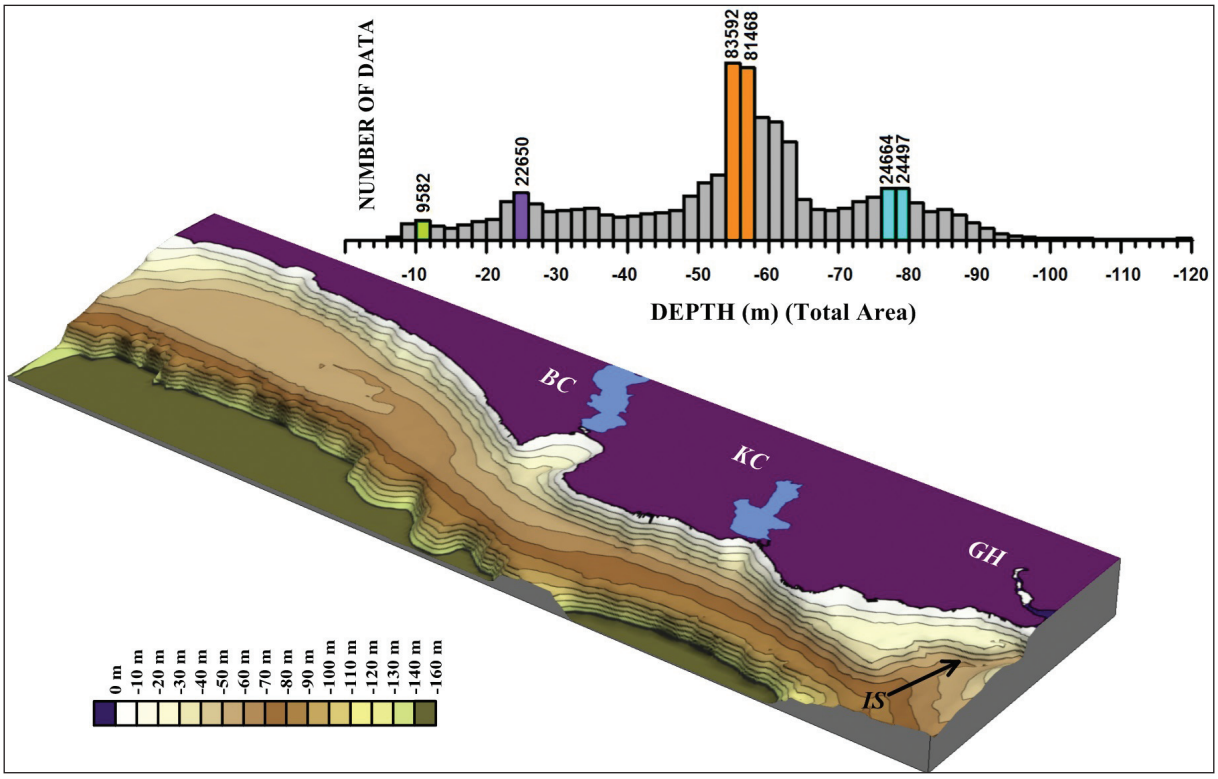

Figure 4- Total depth prevalence analyses with bar graph of the water depth Frequency distribution based on approximately 178,000 depth measurements. The horizontal axis is the measured depths from the echosounder; the vertical axis is the number of depth measurement for a given bin (bin size is 2 m.). From statistical point of view, the most significant depth intervals occur between -10 m and -12 m, -24 m and -26 m, -54 and -58 m and -76 and -80 m. BC: Büyükçekmece, KC: Küçükçekmece, GH: Golden Horn and IS: İstanbul Strait (Bosphorus).

and U2) were identified within the five sedimentary seismic units (S1-S5) overlying the acoustic basement (AB) (Figures 2 and 5).

The beds of the acoustic basement underlying the sedimentary units (S1-S5) dip towards southeast and have strong and irregular surfaces reflection configuration (Figure 5). The top of the sedimentary acoustic basement (Figures 5 and 6) is an erosional unconformity (U1) formed during the Last Glacial Maximum (LGM) period. The oldest seismic unit (S5; Layer-D) fills the paleo-depression and channel over the unconformity surface U1 (Figures 3, 5 and 6). Unit S5 is generally represented by a strong chaotic reflection, having internal reflection characteristics indicative of relatively coarse-grained sediments over the top of the AB in depression. Gravelly and well-rounded sediments (Unit-S5) might have been concentrated under the winnowing and washing processes of the high energy (regressive) conditions during the Last Glacial regressive period. Another prominent unconformity surface U2 occurs at the top of the Unit S5. This unconformity is partially erosional and was formed during the post-glacial wet period. It is overlain by the onlapping transgressive unit S4 and S3 with the well-developed bioherms at the bottom of Unit S4 and top of Unit S5 (Hiscott et al., 2007, Çağatay et al., 2009 and Eriş et al., 2011) (Figure 6).

Mud dominated and weakly stratified S4, S3, S2, and S1 units above the unconformity surfaces (U1 and U2) consist of weak-reflection and acoustically transparent internal structure. Moreover, these units are separated by conformable R3, R2 and R1 reflectors from each other, respectively (Figure 5). Units S3, S2 and S1 are significantly thicker at the eastern depression of the shelf and on the margins. These units thin considerably as close to the shore and on the south side of the shelf.

Sedimentary deposits overlying the regional unconformity surface (U1) are identified as Holocene sediment having calibrated ages younger than 9575 ± 115 Cal yr BP for which the total thickness along the shallow seismic reflection lines was calculated and

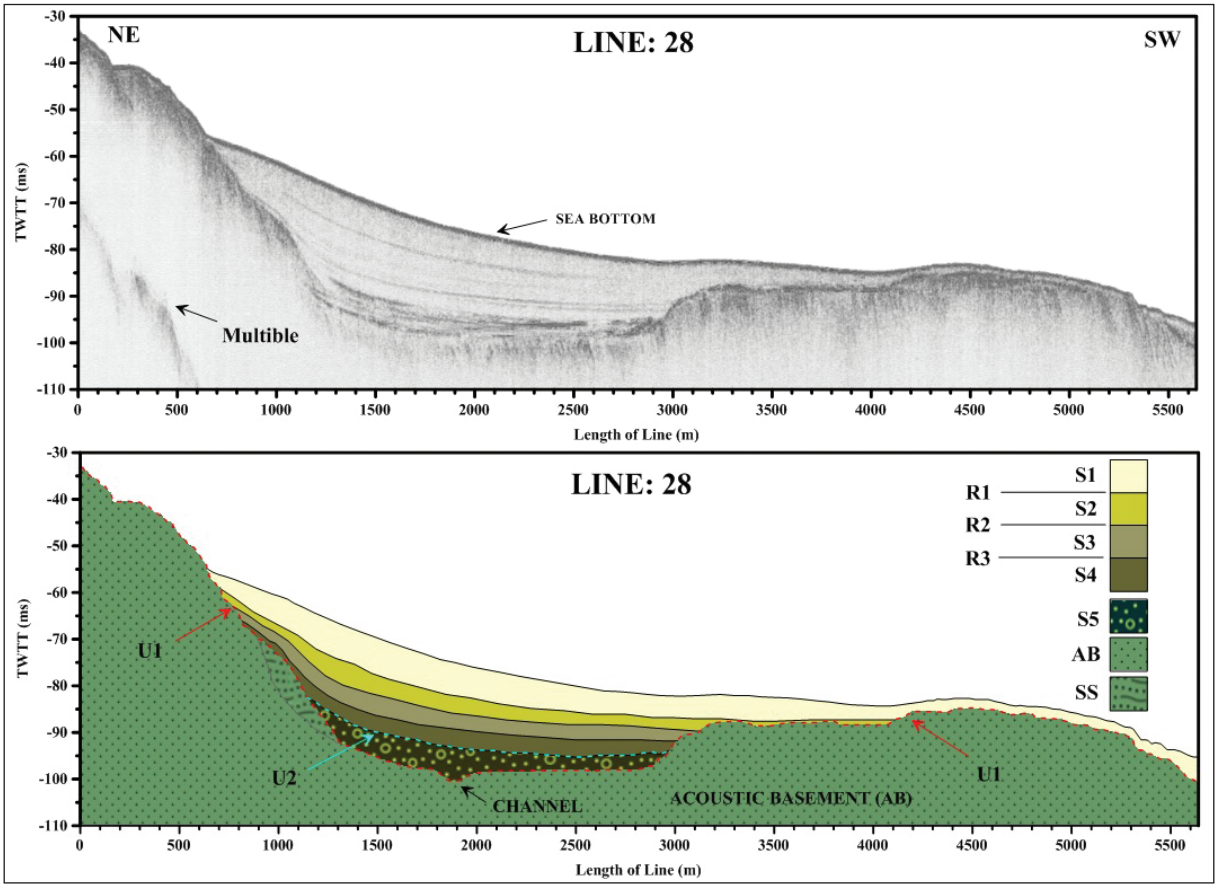

Figure 5- High resolution seismic section from Line-28 (top). Seismic stratigraphy and interpretation of the Line-28 (bottom). Location of the line is given in Fig. 2. S1, S2, S3, S4 and S5 are the main sedimentary units; SS is a kind of slumping/sliding deposit; AB is Acoustic Basement; R1, R2 and R3 are the main transgressive and U1 and U2 are erosional surfaces.

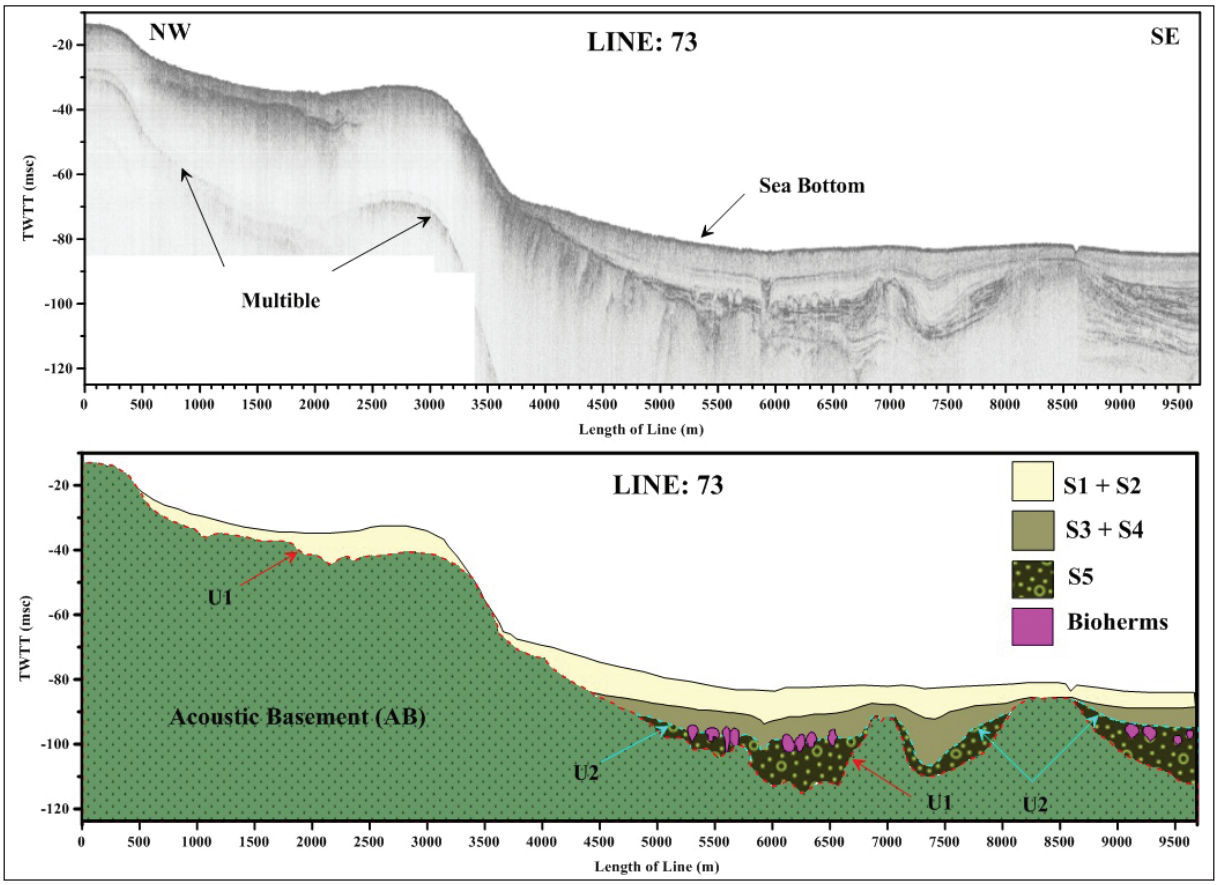

Figure 6- High resolution seismic section from Line-73 (top) and the interpreted section (bottom). Location of the line is given in figure 2. S1, S2, S3, S4 and S5 are the main sedimentary units.

mapped (Figures 3 and 5). Figure 7 shows the thickness map of Holocene sediments over the acoustic basement. Thickness variations in sediment cover are strongly controlled by the sediment sources, sedimentary processes and topography of the underlying erosional surface. Areas of thick sediment deposition generally occur over localized bedrock troughs, near the coastal zone, at the edge of the shelf and at the Istanbul Strait-Marmara Sea junction (Figure 7). Notable examples of 10 to 15 m thick sedimentary deposition occur filling depressions in the eastern and central part of the area. The thickest deposits (15-30 m) are located at the inner part of the Büyükçekmece Bay and western depressed mid-shelf area (Figure 7). Sediment cover is thin in most of the central part where this part is not completely devoid of sediment (Figure 7). High resolution seismic reflection profiles indicate that the Holocene sediments with less than 5 m thickness are common throughout the study area. There are some localities where the sediment cover drops down to less than 2 m thick due to probable sediment removal by bottom currents (Figure 7).

3.3. Acoustic Basement Topography and Terraces

From the shallow seismic reflection lines (80 lines) collected from the study area, only those standing perpendicular to the shore and those parallel to one another (40) lines) were selected for the morphological analysis of the acoustic basement. The sub-bottom morphology of the shelf, most probably controlled by the North Anatolian Fault (NAF) and its side and secondary effects in the south of the study area, is narrowing and deepening from west to east direction (Figure 8).

The frequency distribution of the measured depths was plotted by using 2 m wide depth bins (Figure 8). The depth frequency histogram optimally separates five modes indicating presence of 3 distinct terraces along the shelf. From figure (8), it is clear that the most significant depths occur between "-78 and -80 m" (-79 ± 1 m; blue area), "-58 and -62 m" (-60 ± 2 m; red area) and "-28 and -32 m" (-30 ± 2 m; green area) intervals of the acoustic basement. The T2 terrace

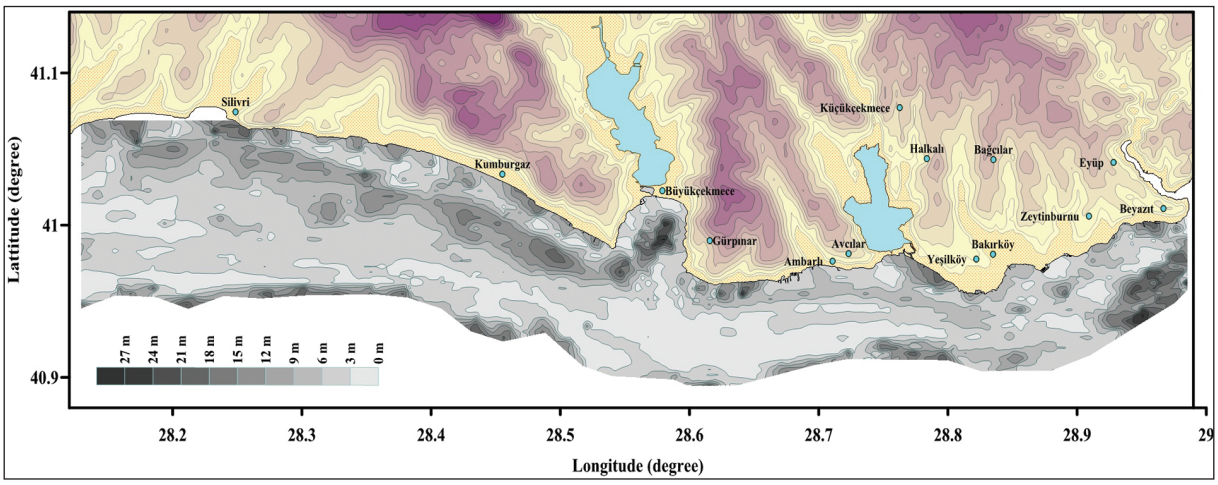

Figure 7- Coastal topography and total Late Quaternary sediment thickness of the northeastern Marmara shelf.

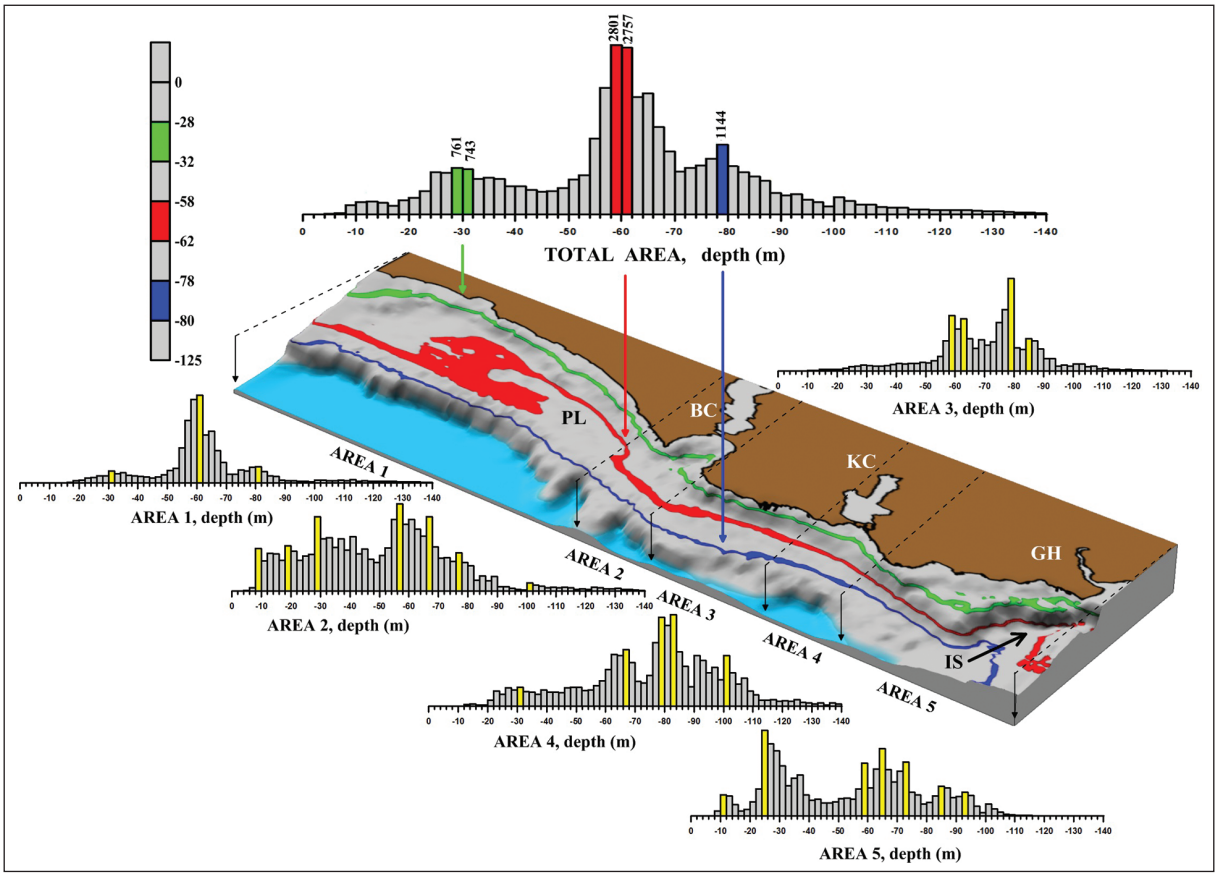

Figure 8- Total depth prevalence analyses with bar graph of the acoustic basement Frequency distribution of the terrace depths based on approximately 12579 samples. The horizontal axis is the measured depths from the reconstructed seismic sections; the vertical axis is the number of depth measurement for a given bin (bin size is 2 m.). From statistical point of view, the most significant terraces occur at T1 (-78 m to -80 m), T2 (-58 m to -62 m) and T3 (-28 m to -32 m). Depth prevalence analyses of the five different parts of the acoustic basement (Areas 1-5) with bar graphs are also given in this figure. BC: Büyükçekmece, KC: Küçükçekmece, GH: Golden Horn, IS: İstanbul Strait (Bosphorus) and PL: Paleo-Lagoon.

located between -58 and -62 m water depths covers the widest and most significant area along the eastern and central mid-shelf (Figure 8). These terraces are also clearly identified on the seismic reflection profiles (and histogram) and labelled T1 (blue), T2 (red) and T3 (green) respectively (Figures 8 and 9).

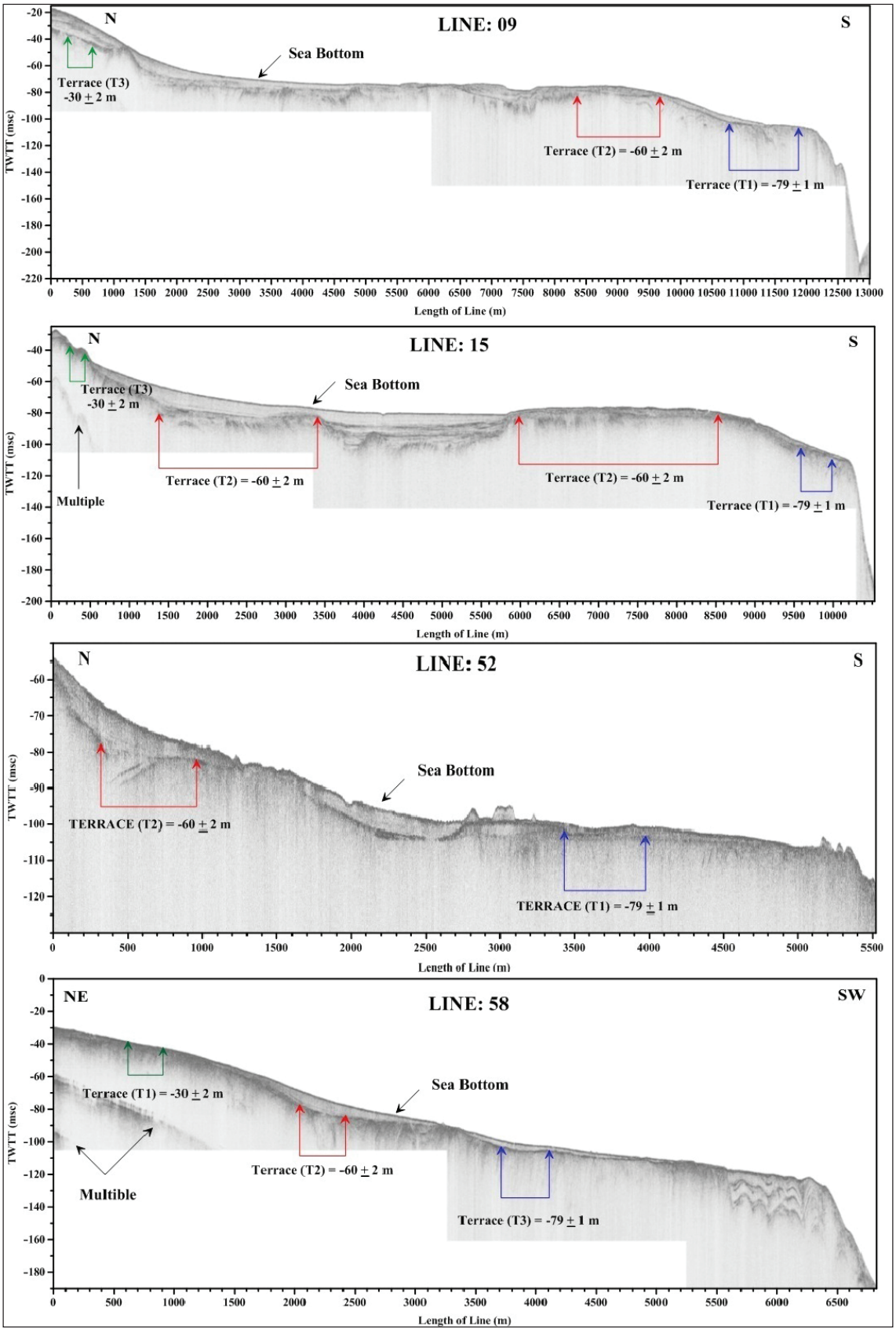

Figure 9- High resolution seismic sections (Lines 15, 52 and 58) and terraces locations. Location of the lines are given in figure 2.

In order to investigate the morphological properties of the sub-bottom in detail, the study area is divided into five different sectors (A1-A5) and bar-graphs of depth values corresponding to these sectors are prepared and separately processed (Figure 8). Morphological characteristics of each shelf sector are considerably different from each other, considering their structural characteristics, distance to NAF, coastal morphology, current system and features of coastal sedimentary processes. The presence of terraces and their depths were identified at -85 m (Çağatay et al 2009, 2003; Polonia et al., 2004; Eriş et al., 2007, 2008; McHugh et al., 2008), -80 m (Kuprin et al., 1974; Shimkus et al., 1980; Dimitrov, 1982; Ballard et al., 2000) and-65 m (Çağatay et al., 2009, 2003; Newman, 2003; Polonia et al., 2004; Eriş et al., 2007, 2008; McHugh et al., 2008) in previous studies. The main reason for these differences may be due to that fact that the seismic reflection data analysed belong to different areas of the Sea of Marmara which could have been affected by different uplift-subsidence rates.

3.4. Lithostratigraphy, Chronostratigraphy and Geochemistry

Four different chronostratigraphic sedimentary layers (A, B, C and D) are distinguished over the acoustic basement (AB) in the cores (Figure 3). Layer-A represents the youngest top sedimentary layer (younger than 575 ± 75 Cal yr BP) and has characteristics of marine deposits (Figure 3). This layer consists of three different sub-layers (A1, A2, and A3) based on the color variations and TOC contents (Figure 3). Dark olive green and brownish homogeneous mud layers (A1) have a maximum of 12 cm thickness at the top of the cores (St-5, St-9, St-11, St-13, St-14 and St-15; Figure 2) and has the lowest TOC content (0.5 wt %; Figure 3). These sediments could be provided by slide and slump of coastal cliffs which are observed along the coastal areas of the studied shelf (Ergintav et al., 2011). In some places, at the bottom of this sub-layer, dark gray to black colored sediments (A2) are present as seen in cores St-1, St-2, St-7, St-8, St-10 and St-12 (Figure 2). These sediments have homogeneous to finely-laminated internal structure (maximum 15 cm thick) and higher TOC contents (1.1 wt %; Figure 3). Sub-layer A3 consists of gray, finely laminated muddy sediments (A3) which are sampled from cores St-7, St-8, St-10 and St-12 and has relatively lower TOC value (0.94 wt %; Figure3) than that of the upper sub-layer (A2).

Layer-B has irregular top and bottom boundaries. It is observed in the cores St-6, St-7 and St-8. Layer B has a high amount of partially eroded *Lithothamnium* grains, carbonate coated terrigenic and biogenic grains and carbonate nodules in dark green muddy matrix. Layer B is dated as 575 ± 75 Cal yr BP (Figure 3). These kinds of sediment mixtures are approximately 22 cm thick in the cores. *Lithothamnium* is reported to dwell in shallow-water areas with sandy and rocky bottoms (Milliman et al., 1972; Campbell, 1982; Alavi et al., 1989). Although both warm and cold marine conditions may provide appropriate environmental conditions for growth of coralline algae, Ergin et al. (1991) noted that most of these organisms live in warm and saline waters in tropical and sub-tropical zones.

Layer-C is made up of as much as 130 cm thick silt dominated and well stratified olive gray sediments which have some micro-sized silt lenses with mica flakes. Layer C is separated into four different sub-layers. Sub-layers C1 through C4 are dated as 1925 ± 115, 3855 ± 165, 5440 ± 140 and 7620 ± 100 Cal yr BP, respectively (Figure 3). Pelecypods (C1 and C3), gastropods (C4) and worm tubes (C2) are observed in the silty muddy matrix at different locations of these sub-layers (Figure 3).

The location of core St-5 on seismic reflection Line-44 is shown in figure 2. This core location is selected for sampling the oldest Holocene sediments (Layer-D) which are deposited over the acoustic basement (AB; Oligocene-U. Eocene) of the northern Marmara shelf. Layer-D, which is dated as 9575 ± 115 Cal yr BP, is deposited over the erosional surface (U1) of the acoustic basement (AB) and composed of washed rounded gravel-sized terrigenic and biogenic grains without matrix in cores St-3 and St-5 (Figures 2 and 3). The presence of the same kinds of sediments and interpretation of their depositional patterns in İzmit Bay (eastern Marmara Sea) were previously discussed by Polonia et al. (2004).

During the deposition of the sediments along the northeastern shelf of the Marmara Sea, sedimentation rates ranged from 0.02 m/kyr to 0.34 m/kyr. The high sedimentation rates are representative of the areas where the water from the coastal rivers (with highly suspended sediments during the flood time) enter into the Marmara Sea and the suspended sediments are rapidly flocculated and then deposited on sea floor during the Holocene.

Bivalve, gastropod and *Lithothamnium* oxygen isotope and pore water salinity values are plotted on the oxygen isotope ratio-salinity diagram of Rank et

al. (1999) in figure 10. Pore water data plot close to the oxygen isotope-salinity line, with two samples each located in the Marmara Sea and the Black Sea sectors. However, a gradual increase of salinity with time are not completely conformable with bivalve, gastropod and *Lithothamnium* ages. This discrepancy may be due to the "vital" effects on the oxygen isotope composition of bivalve, gastropod and *Lithothamnium* caused by growth rate, size and age (Wefer and Berger, 1981). Despite this discrepancy, the bivalve, gastropod and *Lithothamnium* data suggest that the transition from brackish water conditions to the present day marine conditions in the Marmara Sea took place sometime between 5400 and 3800 Cal yr BP.

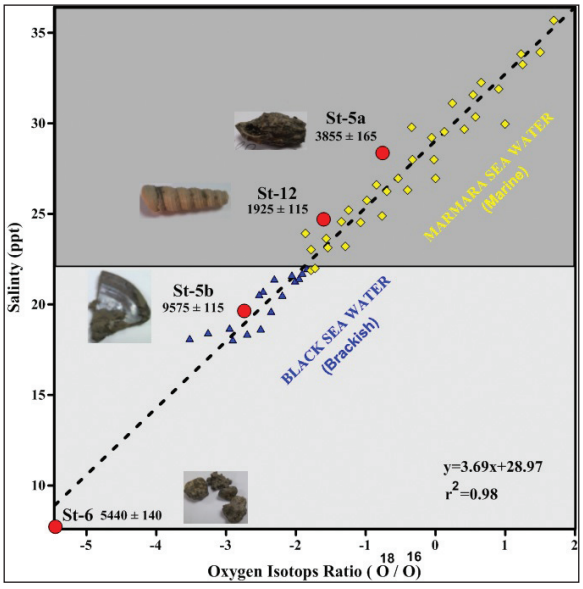

Figure 10- Relationship between salinity (‰) and the Oxygen Isotops Ratio ($^{18}O/^{16}O$) in the Marmara Sea, Black Sea (adapted from Rank et al., 1999) and along the cores.

4. Discussion

In this section, we discuss the ages of the terraces (T1, T2, T3) and the water exchanges between the Mediterranean, the Marmara Sea and the Black Sea, based on the high-resolution shallow seismic reflection profiles, sediment cores and post-glacial sea-level curves (Figures 3, 8 and 11).

It is generally accepted that the minimum sill depths of the bedrocks in the Çanakkale and İstanbul Straits have controlled the connections between the Aegean Sea, Marmara Sea and Black Sea (e.g., Eriş et al., 2008, Çağatay et al., 2009, Gökaşan et al., 2010). Previous studies suggest that the Çanakkale (Yaltırak et al., 2002) and İstanbul Straits and shelf of the Marmara Sea were exposed during the LGM, with fluvial erosion lowering the depths of the straits (Eriş et al., 2007, 2008; McHugh et al., 2007; Çağatay et al., 2009; Gökaşan et al., 2010) and shelf areas. Sea-level fluctuations in the Aegean Sea, Marmara Sea and Black Sea were associated with the global climate and sea level change, size of the drainage basins and depth of the straits. Sea-level started to rise, during the post-glacial warm and wet periods (WWP) after the last glacial maximum (LGM), which took place after 22 Cal kyr BP (Gornitz, 2009) (Figure 11). Before the beginning of the late glacial period, Aegean Sea level stood at -120 m, Marmara Sea level around -105 m and the Black Sea level between -60 m and -90m (Eriş et al., 2011).

In today's climatic and oceanographic conditions of the Aegean, Marmara and Black Seas, the only relatively semi-enclosed Black Sea has positive freshwater balance because of the high ratio of drainage to surface area (D/S) of the Black Sea (4 times greater than Marmara Sea and 2 times greater than the Mediterranean Sea). This provides the Marmara Sea and Aegean Sea with a Black Sea outflow through the İstanbul and Çanakkale straits. A one-way outflow from the Black Sea most likely operated during the late glacial due to the glacier melt waters. Such a continuous Black Sea outflow hypothesis during the late glacial and early Holocene is supported by our study as well as by some previous studies (Degens and Ross 1974; Lane-Serff et al. 1997; Aksu et al., 2002c; Hiscott et al., 2002). However, some other researchers have argued an evaporative drawdown of the Black Sea level during the late-glacial period (Ryan et al., 1997; Ballard et al., 2000).

As a result, there is no consensus among the scientists about the timing of the water connections between the Aegean Sea and Black Sea during the post glacial period. The water-level would have changed at different rates in different basins, depending on the climate, latitude of the basin, the values of D/S ratio and the connection with the local basins. The first sea-level rise period started after the LGM (22 Cal kyr BP) during the late glacial (Figures 11 and 12 A). The level of the Black Sea reached the minimum depth of İstanbul Strait (around -30m; Major et al., 2006) between the 13.7-22 Cal kyr BP (Figures 11 and 12 B), which could have then started a one-way flow

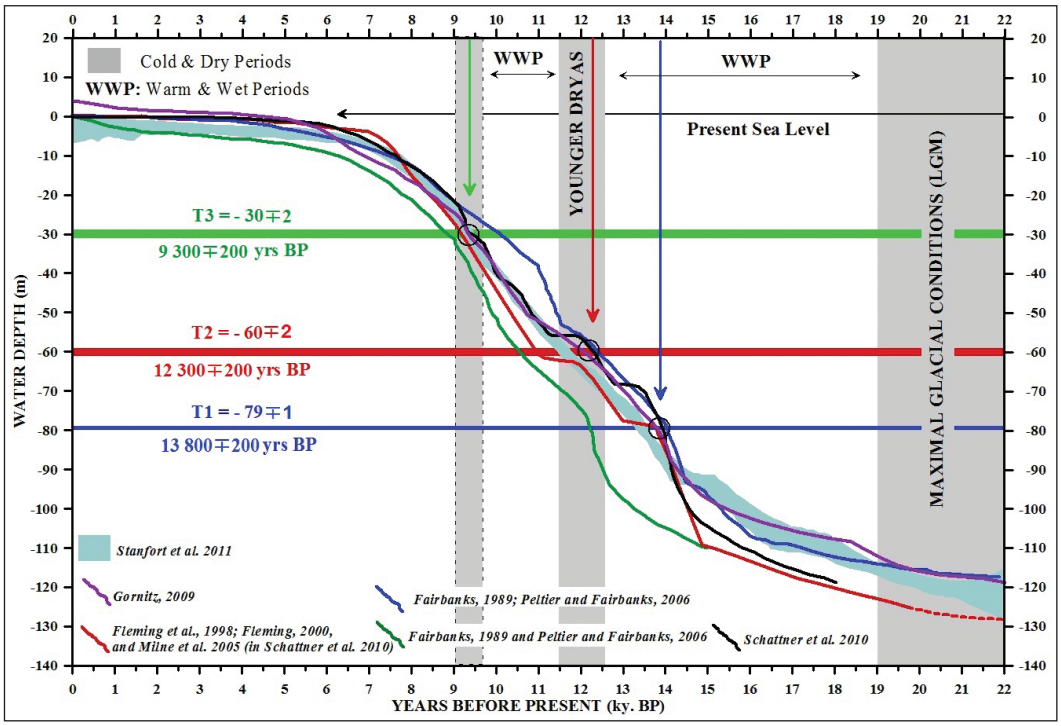

Figure 11- Sea-level rise (depth-time) since the end of the last glacial maximum (Fairbanks, 1989, Fleming et al., 1998, Fleming, 2000, Gornitz, 2009, Milne et al., 2005, Peltier and Fairbanks, 2006, Schattner et al., 2010, Stanford et al., 2011 and http://www.globalwarmingart.com) and terrace depths, LGM: Last Glacial Maximum. Colored arrows and black circles indicate times and depths of the three different terraces.

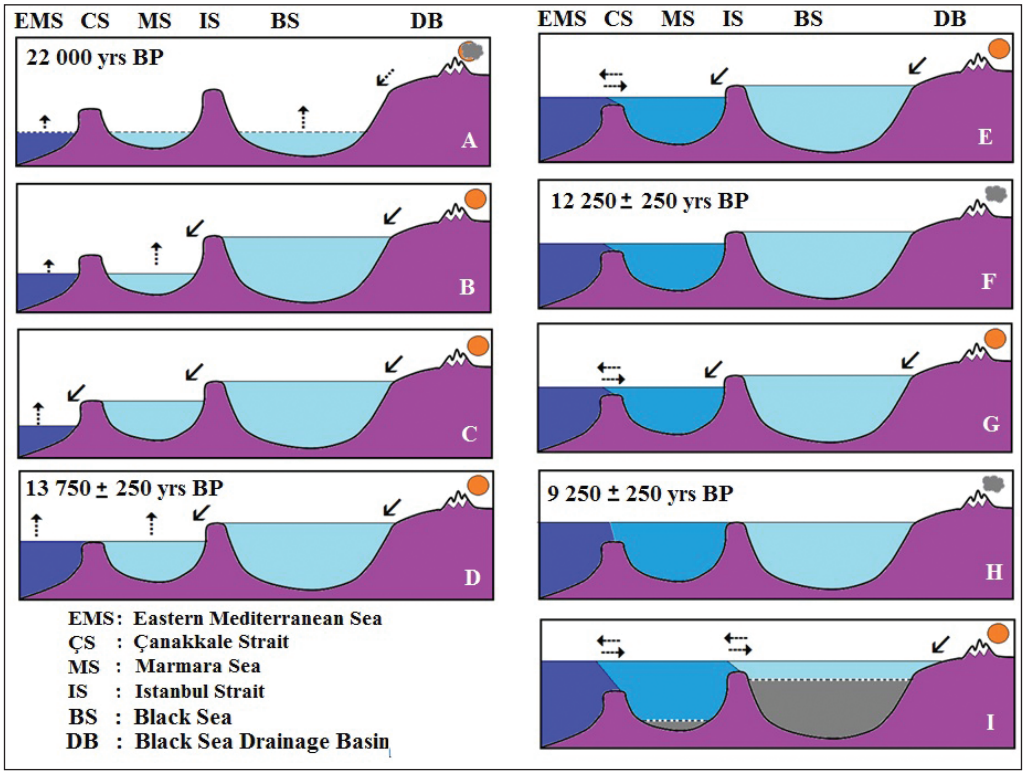

Figure 12- Sketch of Late Quaternary sea-level changes and water exchange among the Marmara, Mediterranean and Black Seas, based on interpretations of seismic reflection profiles, subbottom topography and previous sea-level change curves (phases A to I).

into the Marmara Sea along the İstanbul Strait (Figure 12 B). At the end of this one-way flow regime from Black Sea to Marmara Sea, Marmara Sea should have filled with fresh Black Sea water to the sill depth of the Çanakkale Strait during the first WWP (Figure 12 B). This one way flow regime should have continued until the global sea level in the Aegean Sea reached to the sill depth of Çanakkale Strait (Figure 12 C and D). Afterwards, the Marmara Sea level would rise in tandem with global sea level (Figure 12 D).

First terrace of the Marmara Sea (T1) was formed by truncation of the Marmara Sea shelf by the wave and current action at the sill depth of Çanakkale Strait (i.e., at -79 ± 1 m) around 13.7 Cal kyr BP when the Marmara Sea was fresh-brackish water lake during the time interval for establishing the first two way connection between Aegean Sea and Marmara Sea (Figures 8, 11 and 12 E). It was the result that the depth of the T1 terrace was controlled by the depth of the Çanakkale Strait. However, when the previous studies were examined, it was observed that the depth of the Çanakkale Strait varied between -65 m and -85 m (Smith et al., 1995; Ryan et al., 1997; Hiscott et al., 2002, 2008; Yaltırak et al., 2002; Aksu et al., 2002*c*; Polonia et al., 2004; Major et al., 2006; Gökaşan et al., 2008; Eriş et al., 2007, 2008; McHugh et al., 2008; Çağatay et al., 2000, 2003, 2009). It has been reported by Çağatay et al. (2000) that the Marmara basin was last inundated by Aegean waters around 12 Cal kyr BP. Areal distribution of the T1 along the slope of the region are given in figure (13 A). Despite the suggestion of Ryan et al. (2003) and Ryan (2007) that the amount of evaporation in the Black Sea kept the water level below the sill of İstanbul Strait during that time, we advocate that the waters produced by glaciers melting during the warm period kept the Black Sea level around the sill depth of İstanbul Strait during the late glacial period.

Truncation of the terrace T1 was completed along the northern Marmara shelf and the two-way flow regime established between the Aegean Sea and the Marmara Sea after 13.7 Cal kyr BP (Figures 12 E). Subsequently, the density stratification and suboxic to anoxic bottom conditions gradually established in the Marmara Sea after the Aegean Sea (Mediterranean Sea) connection. These conditions led deposition the sapropel and sapropelic layers dated as ~12-7 and 5-3 Cal kyr BP in the Marmara Sea cores (Çağatay et al., 1999; 2000, 2009, 2015; Tolun et al., 2002; Aksu et al., 2002*c* and 2008). The cold and dry period of Younger Dryas (YD) was period of sea level still stand (Fairbanks, 1989), that resulted in slow down of the unidirectional flow from Black Sea to Marmara Sea and the bidirectional flow from Aegean Sea to Marmara Sea (Figure 11; 12F) (Lane-Serff et al., 1997). The Marmara Sea level during the YD, in tandem with global sea level, was around -60 m according to the global sea level curves. This was the period when the second terrace (T2) was truncated at around -60 ± 2 m by strong current and wave action (Figures 11, 12 F). Throughout this period, the Black Sea water must have been fresh and that of the Marmara Sea partially brackish. This second terrace at -60 ± 2 m water depth is statistically the most significant and morphologically the most common of all the terraces along the northern Marmara shelf (Figures 8, 11). The depth of the Marmara Sea terrace (T2) was claimed to be around -65 m in previous studies (in Newman, 2003; Polonia et al., 2004; Eriş et al., 2007, 2008; McHugh et al., 2008; Çağatay et al., 2003, 2009). The areal distribution of terrace T2 and the presence of a paleo-lagoon along the northern shelf is shown in figure (13 B). Paleo-lagoon and some coastal lakes probably had been filled with the melt fresh waters at the end of this period. Also, bioherms probably developed over the unconformity surfaces (U1) around the western side of the Marmara Sea-İstanbul Strait junction (Figure 6). The YD age of terrace T2 is supported by radiocarbon dating of a broad wave-cut terrace in the Princes' Islands shelf (Eriş et al., 2010).

Some researchers have proposed a gradual connection between the Marmara Sea and Black Sea (e.g., Aksu et al., 2002*a, b*; Hiscott et al., 2002, 2007), whereas others have suggested an abrupt connection (Ryan et al., 1997, 2003; Major et al., 2002, 2006; Myers et al., 2003; Siddall et al., 2003). During the early Holocene warm and wet period (~11.7-9.3 Cal kyr BP) after the Younger Dryas, the sea-level gradually rose to the level of the İstanbul Strait's sill and the first Mediterranean transgression of the Black Sea took place at around 9.3 Cal kyr BP (Major et al., 2002; Ryan, 2007). A two-way flow connection was established between the Aegean Sea and Marmara Sea via the Çanakkale Strait during this WWP (Figures 12 G and H). Terrace T3 corresponds to the İstanbul Strait's sill depth and was most likely controlled by a short sea level still stand around 9.3 Cal kyr BP (Figures 12 H, 13). However, when the previous studies were examined, it was observed that the depth of the İstanbul Strait varied between -35 m and -45 m (Fairbanks, 1989; Görür et al., 2001; Hiscott et al.,

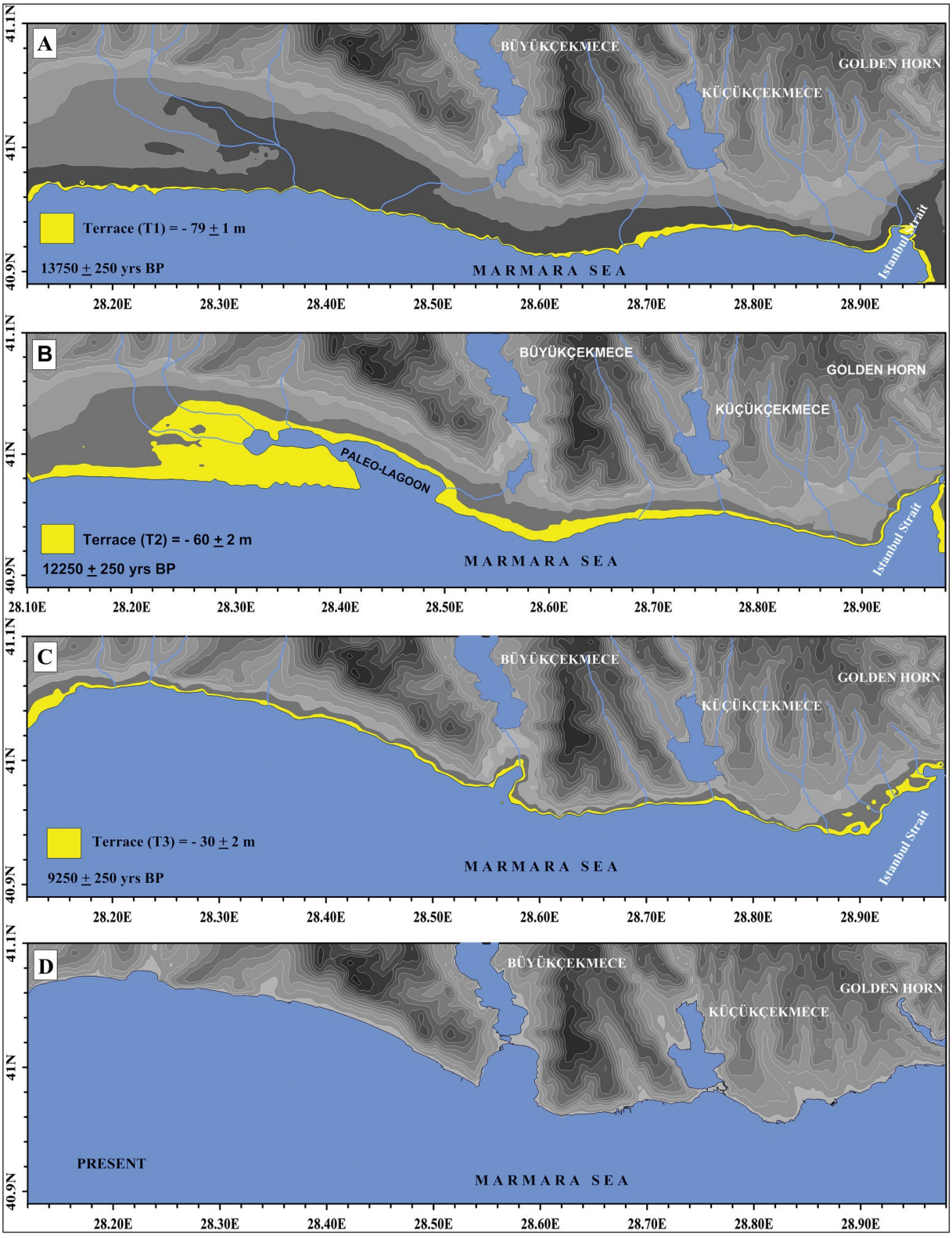

Figure 13- Paleo shorelines along the northeastern Marmara shelf during the low-stand periods of the sea at -78 m to -80 m, -58 m to -62 m, -28 m to -32 m and present condition. Black solid lines represent shore-lines. Coastal drainage networks (blue lines) are given in these figures.

2002; Yaltırak et al., 2002; Aksu et al., 2002*a*; Major et al., 2006; McHugh et al., 2008; Eriş et al., 2007, 2008; Çağatay et al., 2000, 2003, 2009). Areal distribution of the T3 along the shelf of the region are given in figure (13 C).This still stand may have been due to hydraulic conditions between the initially opposing flows of Mediterranean and Black Sea waters and/or climatic causes.

The present day two-way flow system along the straits and anoxic Black Sea bottom conditions were established after 9.3 Cal kyr BP (Figure 12I). Present day geometry of the coastal zone has been shaped after about 6 Cal kyr BP when the sea-level stabilized near the present sea level (Figures 11 and 13 D).

5. Conclusions

By using high resolution shallow seismic reflection data and applying basic seismic stratigraphic techniques, three distinct main boundary reflector surfaces (R1, R2 and R3) and two unconformity surfaces (U1 and U2) were identified among the five sedimentary seismic units (S1-S5) over the acoustic basement (AB).

Four different chronostratigraphic sedimentary layers (A, B, C and D; younger than 9575 ± 115 Cal yr BP) have been distinguished over the acoustic basement (AB) in the Northern Shelf of the Marmara Sea. Total thickness of the Late Quaternary deposits reaches up to 30 m in the eastern depression of the shelf and Büyükçekmece Bay. The central part of the shelf is not completely devoid of sediment, but most of the deposits are less than 2 m thick. Sedimentation rates on the northeastern shelf of the Marmara Sea range from 0.05 m/kyr to 0.34 m/kyr. The distribution of acoustic basement depth values on the density bar-graph shows the presence of three basic terraces (T1, T2 and T3) at depths of -79 ± 1, -60 ± 2 and -30 ± 2 respectively.

The Black Sea level should have gradually increased since the last glacial maximum and one-way flow regime from Black Sea to Marmara Sea should have been established after filling of Black Sea basin due to higher water inputs during the late glacial melt water events. With the Black Sea outflow, the Marmara Sea water level reached the depth of the Çanakkale Strait and established a one-way outflow from Marmara Sea to Aegean Sea (13.7 Cal kyr BP). The one-way flow from Marmara Sea to Aegean Sea continued until the global sea level reached the depth of Çanakkale Strait around 13.7 Cal kyr BP. The depth of the Marmara Sea level stabilized at the sill depth of Çanakkale Strait that controlled the formation of the T1 terrace (at -79 ± 1 m) by wave and current truncation under lacustrine conditions of the Marmara Sea. Subsequent to the marine connection at 13.7 Cal kyr BP, water stratification and anoxic sea bottom conditions were established during this transgressive period.

The overflow from the Black Sea to Marmara Sea was probably gradually stopped and two way flow regime degenerated between the Aegean Sea and Marmara Sea around the 12.3 Cal kyr BP during the Younger Dryas (Fairbanks, 1989) at the end of the first warm and wet period. During the Younger Dryas, the second terrace (T2) might have been truncated around -60 ± 2m depth intervals by strong coastal erosion and sediment reworking processes by the currents and waves during the cold and dry period (Younger Dryas). Throughout this period, the Black Sea water must have been fresh and that of the Marmara Sea partially brackish. Paleo-lagoon and some coastal lakes were developed and filled with the fresh melt waters at the end of this period. Also, bioherms developed over the unconformity surfaces (U1) around the western side of the Marmara Sea-İstanbul Strait junction.

At the end of the Younger Dryas, the sea-level started to rise gradually in the Aegean Sea and Marmara Sea and the two-way flow regime between Aegean Sea and Marmara Sea and one-way flow regime from Black Sea to Marmara Sea were established. Overflow probably gradually stopped from the Black Sea to Marmara Sea and the two-way flow regime re-established between the Aegean Sea and Marmara Sea after the 9.3 Cal kyr BP as a result of the beginning of the second cold and dry period. The sea-level reached -30±2 m (sill depth of the İstanbul Strait) around 9.3 Cal kyr BP when the T3 terrace of the Marmara Sea was formed by wave and current truncation.

The present day two-way flow system along the straits and anoxic Black Sea bottom conditions were established after 9.3 Cal kyr BP. Present day geometry of the coastal zone has been shaped after about 6 Cal kyr BP when the sea-level stabilized near the present sea level.

Acknowledgements

This research was supported by the "Scientific and technical cooperation protocol within the scope of investigating probable faults in land areas of İstanbul and developing landslide detection and monitoring methods through multidisciplinary research of priority landslide areas; 509770" project, funded by Istanbul Metropolitan Municipality (İBB) and the Scientific and Technological Research Council of Turkey (TÜBİTAK) Marmara Research Center (MRC). The authors also express their sincere thanks to the project teams of the İBB-Earthquake and Ground Research Directorate and TÜBİTAK MRC-Earth and Marine Sciences Institute for their kind effort in providing the data during surveys. The authors thank the officers, crew and scientific staff on the R/V Koca Piri Reis (Dokuz Eylül University) and R/V Arar (İstanbul University) for invaluable assistance during a succession of successful cruises. We thank Prof. Dr. Namık Çağatay, Dr. Christopher Sorlien and an anonymous reviewer for valuable suggestions and contributions that improved our paper.

References

Aksu, A.E., Hiscott, R.N., Yaşar, D., Işler, F.I., Marsh, S. 2002*a*. Seismic stratigraphy of Late Quaternary deposits from the southwestern Black Sea shelf: evidence for non-catastrophic variations in sea-level during the last 10,000 years. Mar. Geol. 190, 61–94.

Aksu, A.E., Hiscott, R.N., Mudie, P.J., Rochon, A., Kaminski, M.A., Abrajano, T., Yaşar, D. 2002*b*. Persistent Holocene outflow from the Black Sea to the Eastern Mediterranean contradicts Noah's Flood hypothesis. GSA Today 12 (5), 4–10.

Aksu, A.E., Hiscott, R.N., Kaminski, M.A., Mudie, P.J., Gillespie, H., Abrojano, T., Yaşar, D. 2002*c*. Last glacial–Holocene paleoceanography of the Black Sea and Marmara Sea: stable isotopic, foraminiferal and coccolith evidence. Mar. Geol. 190, 119–149.

Aksu, A.E., Jenner, G., Hiscott, R.N., İşler, E.B. 2008. Occurrence, stratigraphy and geochemistry of Late Quaternary tephra layers in the Aegean Sea and the Marmara Sea Mar. Geol. 252, 174–192.

Alavi, S.N., Ediger, V., Ergin, M. 1989. Recent sedimentation on the shelf and upper slope in the Bay of Anamur, southern coast of Turkey, Mar. Geol.i 89: 29-56. Fli.igel, E. 1978. Mikrofazielle Untersuchungsmethoden yon Kalken. Springer, Berlin, 454 p.

Alpar, B., Yüce, H. 1998. Sea-level variations and their interactions between the Black Sea and the Aegean Sea. Estuar Coast Shelf Sciences, 46, 609-619.

Badley, M.E. 1985. Practical Seismic Interpretation. Prentice-Hall, Englewood Cliffs, N J, 266 p.

Ballard, R.D., Coleman, D.F., Rosenburg, G. 2000. Further evidence of abrupt Holocene drowning of the Black Sea shelf: Marine Geology 170, 253–261.

Beşiktepe, Ş., Sur, H.I., Özsoy, E., Latif, M.A., Oğuz, T., Ünlüata, Ü. 1994. The circulation and hydrography of the Marmara Sea. Prog. Oceanogr. 34, 285-334.

Boggs, S. Jr. 1987. Principles of Sedimentology and Stratigraphy. Macmillan, New York, 784 p.

Brown, Jr., L.F., Fisher, W.L. 1980. Seismic Stratigraphic Interpretation and Petroleum Exploration. AAPG Continuing Education Course Note Series 16, Tulsa, Oklahoma, 125 p.

Campbell, A.C. 1982. The Hamlyn Guide to the Flora and Fauna of the Mediterranean Sea. Hamlyn, London, p. 320.

Çağatay, M.N., Algan, O., Sakınç, M., Eastoe, C.J., Egesel, L., Balkis, N., Ongan, D., Caner., H. 1999. A mid-late Holocene sapropelic sediment unit from the southern Marmara sea shelf and its palaeoceanographic significance, Quaternary Science Reviews 18 (1999) 531-540.

Çağatay, M.N., Görür, N., Algan, O., Eastoe, C., Tchalaliga, A., Ongan, D., Kuhşl, T., Kuşçu, İ. 2000. Late Glacial-Holocene paleoceanography of the Sea of Marmara: timing of connections with the Mediterranean and the Black Sea. Mar. Geol. 167, 191–206.

Çağatay, M.N., Görür, N., Polonia, A., Demirbağ, E., Sakınç, M., Cormier, M.-H., Capotondi, L., McHugh, C.M.G., Emre, Ö., Eriş, K. 2003. Sea-level changes and depositional environments in the İzmit Gulf, eastern Marmara Sea, during the late glacial–Holocene period. Mar. Geol. 202, 159–173.

Çağatay, M.N., Eriş, K., Ryan, W.B.F., Sancar, Ü., Polonia, A., Akçer, S., Biltekin, D., Gasperini L, Görür, N., Lericolaris, G., Bard, E. 2009. Late pleistocene-holocene evolution of the northern shelf of the Sea of Marmara, Mar. Geol. 265, 87-100.

Çağatay, M.N., Wulf, S., Guichard, F., Özmaral, A., Henry, P., Gasperini, L. 2015. Tephra record from the Sea of Marmara for the last 71 ka and its paleoceanographic implications. Marine Geology, 361: 96-110.

DAMOC, 1971. Master plan and feasibility report for water supply and sewerage for Istanbul region. Prepared by the DAMOC Consortium for WHO, Los Angeles, CA, vol. III, part II and III.

Degens, E.T., Ross, A. 1974. The Black Sea-Geology, chemistry, and biology. American Association of Petroleum Geologists, Tulsa, Oklahoma, 633 p.

Dimitrov, P. 1982. Radiocarbon datings of bottom sediments from the Bulgarian Black Sea shelf. Bulg. Acad. Sci. Oceanol. 9, 45-53.

Ediger, V., Okyar, M, Ergin, M. 1993. Seismic stratigraphy of the fault-controlled submarine canyon/valley system on the shelf and upper slope of Anamur Bay, Northeastern Mediterranean Sea. Mar. Geol. 15, 129-142.

EIE, 1993. Sediment data and sediment transport amount for surface water in Turkey. Türkiye Elektirik İşleri Etüd Dairesi Genel Müdürlüğü, Ankara, EIE Publ., No.68. 56 p.

Ergin, M., Bodur, M.N., Ediger, V. 1991. Distribution of surficial shelf sediments in the northeastern and southwestern parts of the Sea of Marmara: Strait and canyon regimes of the Dardanelles and Bosphorus. Mar. Geol. 96, 313-340.

Ergintav, S., Demirbağ, E., Ediger, V., Saatçılar, R., Inan, S., Cankurtaranlar, A., Dikbaş, A., Baş, M. 2011. Structural framework of onshore and offshore Avcılar, ˙Istanbul under the influence of the North Anatolian fault. Geophys. J. Int. 185, 93–105.

Eriş, K.K., Ryan, W.B.F., Çağatay, M.N., Sancar, U., Lericolais, G., Ménot, G., Bard, E. 2007. The timing and evolution of the post-glacial transgression across the Sea of Marmara shelf south of İstanbul. Mar. Geol. 243 (1-4), 57-76.

Eriş, K.K., Ryan, W.B.F., Çağatay, M.N., Lericolais, G., Sancar, Ü., Menot, G, Bard, E. 2008. Reply to Comment on "The timing and evolution of the post-glacial transgression across the Sea of Marmara shelf south of İstanbul" by Hiscott et al., Mar. Geol. 248 228-236.

Eriş, K.K., Çağatay, M.N., Akçer, K., Luca, G., Yosi., M. 2010. Late glacial to Holocene sea-level changes in the Sea of Marmara: new evidence from high-resolution seismics and core studies. Geo-Mar Lett 31:1–18.

Eriş, K.K., Çağatay, M., Sena, A., Gasperini, L., Mart, Y. 2011. Late glacial to Holocene sea-level changes in the Sea of Marmara: new evidence from high-resolution seismics and core studies, Geo-Marine Letters, V:31, N:1, 1-18.

Fairbanks, R.G. 1989. A 17,000 year glacio-eustatic sea-level record: Influence of glacial melting rates on the Younger Dryas event and deep-ocean circulation: Nature, v. 342, p. 637-642.

Fleming, K. M. 2000. Glacial Rebound and Sea-level Change Constraints on the Greenland Ice Sheet. Australian National University. PhD Thesis.

Fleming, K., Johnston, P., Zwartz, D., Yokoyama, Y., Lambert, K., Chappell, J. 1998. Refining the eustatic sea-level survey since the Last Glacial Maximum using far- and intermediate-field sites. Earth Planet. Sci. Lett. 163, 327–342.

Gökaşan, E., Demirbağ, E., Oktay, F.Y., Ecevitoğlu, B., Şimşek, M., Yüce, H. 1997. On the origin of the Bosphorus. Mar. Geol. 140, 183–199.

Gökaşan, E., Ergin, M., Özyalva Ç. M., İbrahim Sur, H., Tur, H., Görum, T., Ustaömer, T., Gül Batuk, F., Alp, H., Birkan, H., Türker, A., Gezgin, E., Özturan, M.., 2008. Factors controlling the morphological evolution of the Canakkale Strait (Dardanelles, Turkey). Geo-Mar Letters 28, 107–129.

Gökaşan E., Tur, H., Ergin, M., Görüm, T., Batuk F.G., Sağcı, N., Ustaömer, T., Emem, O., Alp, H. 2010. Late Quaternary evolution of the Çanakkale Strait region (Dardanelles, NW Turkey): implications of a major erosional event for the postglacial Mediterranean-Marmara Sea connection. Geo-Mar Lett (2010) 30:113-131.

Gornitz, V. 2009. Sea level change, post-glacial. In Encyclopedia of Paleoclimatology and Ancient Environments. V. Gornitz, Ed., Encyclopedia of Earth Sciences Series. Springer, 887-893.

Görür, N., Çağatay, M.N., Emre, Ö., Alpar, B., Sakınç, M., Islamoğlu, Y., Algan, O., Erkal, T., Keçer, M., Akkök R., Karlık, G. 2001. Is the abrupt drowning of the Black Sea shelf at 7150 yr BP a myth? Mar. Geol. 176, 65-73.

Hiscott, A.E., Aksu, R.N, Mudie, P.J, Kaminski, M.A., Abrajano, T., Yaşar, D., Rochon, A. 2007. The Marmara Sea gateway since 16 ky BP: non-catastrophic causes of paleoceanographic events in the Black Sea at 8.4 and 7.15 ky BP. In: Yanko-Hombach, V., Gilbert, A.S., Dolukhanov, P.M. (Eds.), The Black Sea Flood Question. Springer, The Netherlands, 89–117.

Hiscott, R.N., Aksu, A.E, Yaşar, D., Kaminski, M.A., Mudie, P.J., Kostylev, V.E., MacDonald, J.C., İşler, F.I., Lord, A.R. 2002. Deltas south of the Bosphorus Strait record persistent Black Sea outflow to the Marmara Sea since ~10 ka. Mar. Geol. 190:95-118.

Hiscott, R.N., Aksu, A.E., Mudie, P.J. 2008. Comment on "The timing and evolution of the post-glacial transgression across the Sea of Marmara shelf south of Istanbul" by Eriş et al., Mar. Geol. 243, 57–76 Mar. Geol., Volume 248, Issues 3-4, 25 February 2008, Pages 228-236.

http://www.globalwarmingart.com

Kaminski, M.A., Aksu, A.E., Box, M., Hiscott, R.N., Filipescu, S., Al-Salameen, M. 2002. Late glacial to Holocene benthic foraminifera in the Marmara Sea: implications for Black Sea-Mediterranean Sea connections following the last deglaciation. Mar. Geol. 190: 165–202.

Keven, G. 2002. Archaeology: An Introduction. Philadelphia: University of Pennsylvania Press. Pages. 165–167.

Kuprin, P.N., Scherbakov, F.A., Morgunov, I.I. 1974. Correlation, age and distribution of the postglacial continental terrace sediments of the Black Sea. Baltica 5, 241-249.

Lane-Serff, G.F., Rohling, E.J., Bryden, H.L., Charnock, H. 1977. Postglacial connection of the Black Sea to the Mediterranean and its relation to the timing of sapropel formation. Paleoceanography Volume 12, Issue 2. Pages 169–174.

Major, C., Ryan, W., Lericolais, G., Hajdas, I. 2002. Constraints on Black Sea outflow to the Sea of Marmara during the last glacial–interglacial transition. Mar. Geol. 190, 19–34.

Major, C.O., Goldstein S.L., Ryan, W.B.F., Lericolais, G., Piotrowski, A.M., Hajdas, I. 2006. The co-evolution of Black Sealevel and composition through the last deglaciation and its paleoclimatic significance. Quat. Sci. Rev. 25, 2031–2047.

Martin, R. E., Leorri, E., McLaughlin, P.P. 2007. Holocene sea level climate change in the Black Sea: Multiple marine incursions related to freshwater discharge events. 2007 Quaternary International 167-168, 61-72.

Meriç, E., Algan, O. 2007. Paleoenvironments of the Marmara Sea (Turkey) Coasts from paleontological and sedimentological data. Quaternary International 167-168, 128-148.

McHugh, W.D., Hansell, D.A., Morgana, J. A. 2007. Reprint of Dissolved organic carbon and nitrogen in the Western Black Sea. Marine Chemistry 105 (1-2), 140-150.

McHugh, C.M.G., Gurung, D., Giosan, L., Ryan, W.B.F., Mart, Y., Sancar, U., Burckle, L., Çağatay, M.N. 2008. The last reconnection of the Marmara Sea (Turkey) to the World Ocean: a paleoceanographic and paleoclimatic perspective. Mar. Geol 255 (1-2), 64-82.

Milliman, J.D., Weiler Y., Stanley D.J. 1972. Morphology and carbonate sedimentation on shallow banks in the Alborian Sea. In: D.J. Stanley (Editor), The Mediterranean Sea A Natural Sedimentation Laboratory. Dowden, Hutchinson and Ross, Stroudsburg, Pa., 241, 259 p.

Mitchum, R.M., Vail, P.R., Sangree, J.B. 1977. Seismic stratigraphy and global changes of sea level, part 6: Stratigraphic interpretation of seismic reflection patterns in depositional sequences. In: C.E. Payton (Editor), Seismic Stratigraphy--Applications to Hydrocarbon Exploration. AAPG Mem., 26: 117-133.

Myers, P.G., Wielki, C., Goldstein, S.B, Rohling, E.J. 2003. Hydraulic calculations of postglacial connections between the Mediterranean and the Black Sea. Mar. Geol. 201, 253-267.

Newman, K.R. 2003. Using Submerged Shorelines to Constrain Recent Tectonics in the Marmara Sea, Northwestern Turkey. Department of Geology, Senior Thesis, Smith College. 49 pp.

Oğuz T., Özsoy E., Latif M., Sur H.I., Ünlüata Ü. 1990. Modeling of hydraulically controlled exchange flow in the Bosphorus Strait. J. Phys. Oceanogr., 20: 945-965

Okyar, M., Ediger, V., Ergin, M. 1994. Seismic stratigraphy of the southeastern Black Sea shelf from high-resolution seismic records. Mar. Geol., Volume 121, Issues 3-4, November 1994, Pages 213-230.

Özsoy, E., Di Iorio, D., Gregg, M., Backhaus, J.O. 2001. Mixing in the Bosphorus Strait and the Black Sea continental shelf: observations and a model of the dense water outflow J. Mar. Syst., 31 (2001), pp. 99-135

Peltier, W.R., Fairbanks, R.G. 2006. Global glacial ice volume and Last Glacial Maximum duration from an extended Barbados sea level record. Quaternary Science Reviews 25 (23-24), 3322-3337.

Polat, Ç., Tuğrul, S. 1996. Chemical exchange between the Mediterranean and Black Sea via the Turkish Straits. In: Briand, F. (Ed.), Dynamics of Mediterranean Straits and Channels. Bulletin de l'Institut Oce.anographique, Monaco, Special No. 17, CIESME Science Series 2, 167-186.

Polonia, A., Gasperini, L., Amorosi, A., Bonatti E., Bortoluzzi, G., Çağatay, N., Capotondi, L., Cormier, M.H., Görür, N., McHugh, C., Seeber, L. 2004. Holocene slip rate of the North Anatolian Fault beneath the Sea of Marmara. Earth Planet. Sci. Lett. 227, 411–426.

Rank, D., Özsoy, E., Salihoğlu I. 1999. Oxygen -18, deuterium and tritium in the Black Sea and the

Sea of Marmara. J. Environ. Radioact. 43, 231-245.

Ryan, W.B.F. 2007. Status of the Black Sea Flood hypothesis. Yanko-Hombach, V., Gilbert, A.S., Panin, N., Dolukhanov, P. (Edit.), The Black Sea Flood Question-Changes in Coastline, Climate and Human Settlement, Springer, Dordrecht, 63-88.

Ryan, W.B.F., Pitman III, W.C., Major, C.O., Shimkus, K., Moskalenko, V., Jones, J.A., Dimitrov, P., Görür, N., Sakınç, M., Yüce, H. 1997. An abrupt drowning of Black Sea shelf. Mar. Geol. 138, 119–126.

Ryan, W.B.F., Major, C.O., Lericolais, G., Goldstein, S.L. 2003. Catastrophic flooding of the Black Sea. Annual Review of Earth and Planetary Sciences 31: 525-554.

Sangree, J.B., Widmier. J.M. 1977. Seismic stratigraphy and global changes of sea level, part 9: Seismic interpretation of clastic depositional facies. In: C.E. Payton (Editor), Seismic Stratigraphy--Applications to Hydrocarbon Exploration. AAPG Mem., 26: 165-184.

Schattner U., Lazar M., Tibor G. 2010. Filling up the shelf – A sedimentary response to the last post-glacial sea rise. Marine Geology 278: 165–176.

Shimkus, K.M., Evsyukov, Y.D., Solovjeva, R.N. 1980. Submarine terraces of the lower shelf zone and their nature. In: Malovitsky, Y.P., Shimkus, K.M. (Eds.), Geological and Geophysical Studies of the Pre-Oceanic zone. P.P. Shirshov Inst. Of Oceanology Acad Sci USSR, Moscow, pp 81-92.

Siddall, M., Rohling, E.J., Almogi-Labin, A., Hemleben, Ch., Meischner, D., Schmelzer. I. Smeed. D.A. 2003. Sea-level fluctuations during the last glacial cycle. Nature 423, 853-858.

Smith, A. D., Taymaz, T., Oktay, F., Yüce, H., Alpar, B., Başaran, H., Jackson, J. A., Kara,S., Şimşek, M. 1995. High-resolution seismic profiling in the Sea of Marmara (northwest Turkey): Late Quaternary sedimentation and sea-level changes. Geological Society of America Bulletin, August 1995 923-936

Stanford, J. D., Hemingway, R., Rohling, E. J., Challenor, P. G., Medina-Elizade, M., Lester, A. J. 2011. Sea-level probability for the last deglaciation: A statistical analysis of far-field records, Global Planet. Change, 79, 193–203.

Stuiver, M., Reimer, P.J. 1993: Extended 14C data base and revised CALIB 3.0 14C age calibration program . Radiocarbon 35, 215-230

Tolun, L., Çağatay, M. N., Carrigan, W. J. 2002. Organic geochemistry and origin of late Glacial-Holocene sapropelic layers and associated sediments in Marmara Sea, Mar. Geol., 190, 47 – 60

Ünlüata Ü., Oğuz T., Latif M., Özsoy E. 1990. On the physical oceanography of the Turkish Straits. *In*: Pratt L.J. (ed.). The physical oceanography of sea straits, Kluwer Academic Publishers, Boston, pp 25-60.

Vail, P.R., Mitchum, Jr.R.M., Thompson, S.III. 1977. Seismic stratigraphy and global changes of sea level, part 3: Relative changes of sea level from coastal onlap. In: C.E. Payton (Editor), Seismic Stratigraphy--Applications to Hydrocarbon Exploration. AAPG Mem., 26: 63-81.

Wefer, G., Berger, W.H., 1981. Stable isotopes composition of benthic calcareous algae from Bermuda: Journal of Sedimentary Petrology, v. 51. 0459-0465 p.

Yaltırak, C., Sakınç, M., Aksu, A.E., Hiscott, R.N., Galleb, B., Ülgen, U.B. 2002. Late Pleistocene uplift history along the southwestern Marmara Sea determined from raised coastal deposits and global sea-level variations. Mar. Geol. 190:283-305.